Manganese-mediated C-H bond activation of fluorinated aromatics and the *ortho*-fluorine effect: kinetic analysis by *in situ* infrared spectroscopic analysis and time-resolved methods

L. Anders Hammarback,[a] Amy L. Bishop,[a] Christina Jordan,[a] Gayathri Athavan,[a] Jonathan B. Eastwood,[a] Thomas J. Burden,[a] Joshua T. W. Bray,[a] Francis Clarke,[a] Alan Robinson,[b] Jean-Philippe Krieger,[c] Adrian Whitwood,[a] Ian P. Clark,[d] Michael Towrie,[d] Jason M. Lynam[a]* and Ian J. S. Fairlamb[a]*

[a] Department of Chemistry, University of York, York, United Kingdom, YO10 5DD. Email: jason.lynam@york.ac.uk; ian.fairlamb@york.ac.uk; [b] Syngenta Crop Protection AG, Schaffhauserstrasse, 4332, Switzerland; [c] Syngenta Crop Protection AG, Münchwilen, Breitenloh 5, 4333, Switzerland. [d] Central Laser Facility, STFC Rutherford Appleton Laboratory, Harwell Science and Innovation Campus, Didcot, Oxfordshire, OX11 0QX, United Kingdom.

Supporting Information Available

ABSTRACT: Insight into the factors controlling the site-selectivity of transition metal-catalyzed C–H bond functionalization reactions is vital to their successful implementation in the synthesis of complex target molecules. The introduction of fluorine atoms into substrates has the potential to deliver this selectivity. In this study we employ spectroscopic and computational methods to demonstrate how the "ortho-fluorine effect" influences the kinetic and thermodynamic control of C–H bond activation in manganese(I)-mediated reactions. The C–H bond activation of fluorinated *N,N*-dimethylbenzylamines and fluorinated 2-phenylpyridines by benzyl manganese(I) pentacarbonyl [$BnMn(CO)_5$] leads to the formation of cyclomanganated tetracarbonyl complexes (**2a-b** and **4a-e**), which all exhibit C–H bond activation *ortho*-to-fluorine. Corroboration of the experimental findings with DFT methods confirms that a kinetically controlled irreversible σ-CAM mechanism is operative in these reactions. The addition of benzoic acid results in a mechanistic switch so that cyclomanganation proceeds through a reversible AMLA-6 mechanism (kinetically and thermodynamically-controlled). These stoichiometric findings are critical to catalysis, particularly subsequent insertion of a suitable acceptor substrate into the C–Mn bond of the regioisomeric cyclomanganated tetracarbonyl complex intermediates. The employment of time-resolved infrared spectroscopic analysis allowed for correlation of the rates of terminal acetylene insertion into the C–Mn bond with the relative thermodynamic stability of the regioisomeric complexes. Thus, more stable manganacycles, imparted by an *ortho*-fluorine substituent, exhibit a slower rate of terminal acetylene insertion, whereas a *para*-fluorine atom accelerates this step. A critical factor in governing C–H bond site-selectivity under catalytic conditions is the generation of the regioisomeric cyclomanganated intermediates, rather than their subsequent reactivity towards alkyne insertion.

Keywords: C-H bond activation, catalysis, manganese, site-selectivity, alkynes, pyridines

INTRODUCTION

The transition metal-mediated functionalization of carbon-hydrogen (C–H) bonds is an important method for structural elaboration. Controlling the regioselectivity of such processes ensures that a specific C–H bond within a substrate of interest is activated, especially when the reactions are applied to the synthesis of complex target molecules.[1] A common solution to controlling the regiochemical outcome of the reaction is to employ Lewis basic directing groups which control the coordination of the substrate to a transition metal, ensuring site-specific C–H bond activation.[2] Alternative strategies, without use of metal-directing groups, can influence regioselectivity and provide an alternative route to control chemical synthesis.[3]

The unique properties of the fluorine atom offer interesting opportunities to alter the inherent regioselectivity in C–H bond activation. Fluorinated aromatic (organic) systems often show an increased preference for metal-mediated activation of aromatic C–H bonds *ortho* with respect to fluorine substituents, and this effect is commonly referred to as the "*ortho*-fluorine effect".[4] The *ortho*-fluorine effect has been observed for many transition metal-mediated transformations, both with[5] and without[6] supplementary directing groups.

There is currently no clear mechanistic consensus on the origin of the *ortho*-fluorine effect and the proposals often change with the reaction system. Studies by Eisenstein, Clot and Perutz have shown that the C–M bond strength was stronger *ortho* to the fluorine substituent in a series of *ortho*-selective transition metal mediated (M = Re, Rh, Ir, Ni, Pt, Ta and W) C–H bond activation of fluorobenzenes.[6a-c] In the C–H bond cyclometallation (M = Rh, Ir) of *meta*-substituted 1-phenylpyrazoles, Davies and Macgregor found no correlation between the observed *ortho*/*para*-selectivity and the C–M bond lengths of the resulting metallacycles.[5a] Eisenstein and Perutz have also reported, for Pd-mediated

C–H bond arylation of fluorobenzenes, that the observed *ortho*-preference arises from a lower activation barrier for C–H bond activation.[6d]

In our previous study with Perutz on Pd-mediated C–H bond activation of fluorinated benzylamines (Scheme 1) we showed that the starting Pd-complex, and thus mechanism of C–H activation, had a major impact on the resulting regioselectivity.[5d] Li_2PdCl_4 (S_EAr) exhibited complete *para*-selectivity, while $Pd_3(OAc)_6$ (CMD/AMLA-6) yielded close to the same amount of both regioisomers. Davies and Macgregor additionally revealed that the extent of an inherent *ortho*-preference in the direct C–H bond cyclometallation (M = Rh, Ir) of *meta*-fluorinated 1-phenylpyrazoles depended on whether the reaction was under kinetic or thermodynamic control.[5a] The same effect has also been reported by Jones and Perutz in the Rh-mediated C–H bond activation of fluorobenzenes, where the kinetic and thermodynamic products could be generated depending on reaction temperature.[6e]

There are few studies probing the nature of fluorine-induced regioselectivity in *3d*-metal-catalyzed C–H bond functionalization reactions. One notable exception is the report by Chirik and co-workers on the borylation of fluorinated arenes by a cobalt pincer complex, which demonstrated that the Co–C bond was exceptionally sensitive to *ortho*-fluorine incorporation and provided a thermodynamic driving force for the observed catalytic selectivity.[7] This increased sensitivity offers the potential for *3d*-metals to have a greater intrinsic selectivity for C–H bond activation on the introduction of fluorine into a given substrate.

Manganese carbonyl complexes are of considerable current interest due to their applications in redox-neutral catalytic processes for C–H bond functionalization.[8] Following Chen and Wang's 'breakthrough' study in 2013 on Mn(I)-mediated C–H bond alkenylation of 2-phenylpyridines,[9] these species have demonstrated a significant potential and versatility as Earth-abundant metal catalysts for applied chemical synthesis.[10] The catalytic chemistry is founded in the stoichiometric organometallic chemistry of manganese which has been studied for >40 years and have included extensive work on directed cyclomanganation of aromatic C–H bonds[11,12] and subsequent reactivity of the resulting manganacycles.[12,13]

Manganese carbonyl complexes have been utilized in the study of fluorine-induced regioselectivity. For example, in 1978 Bruce reported an apparent *ortho*-fluorine effect in the Mn-mediated C–H bond activation of fluorinated azobenzene derivatives, generating exclusively the *ortho*-complex.[5b] Liebeskind found a relatively strong *ortho*-preference in the C–H bond cyclomanganation of *meta*-fluorinated acetophenones (4.5:1, *ortho*/*para*), where other substituents exhibited weaker *ortho*-selectivity (OMe, 2.1:1, *ortho*/*para*) to selective formation of the *para*-complex (Me, CF_3, CN).[13a] An *ortho*-fluorine effect has also been reported in Mn(I)-mediated alkenylation of 2-phenylpyridines, where only the C–H bond functionalization *ortho* to fluorine was seen for a *meta*-fluorinated 2-phenylpyridine.[9]

In a recent series of studies, we have described how mechanistic studies on reactions catalyzed by Mn(I) carbonyl complexes can provide unique insight into transition metal-mediated bond activation and formation pathways.[14] Connecting complementary information from time-resolved infra-red spectroscopy on a picosecond to microsecond (ps-μs) timescale, with measurements by NMR and *in situ* IR analysis on *in operando* reactions and calculations using density functional theory (DFT), have enabled the obtention of a comprehensive picture of the steps underpinning C–C bond formation, catalyst activation and deactivation pathways. This approach also allowed for the first experimental observation of the steps underpinning the Concerted Metalation Deprotonation (CMD) reaction to be directly observed.[15]

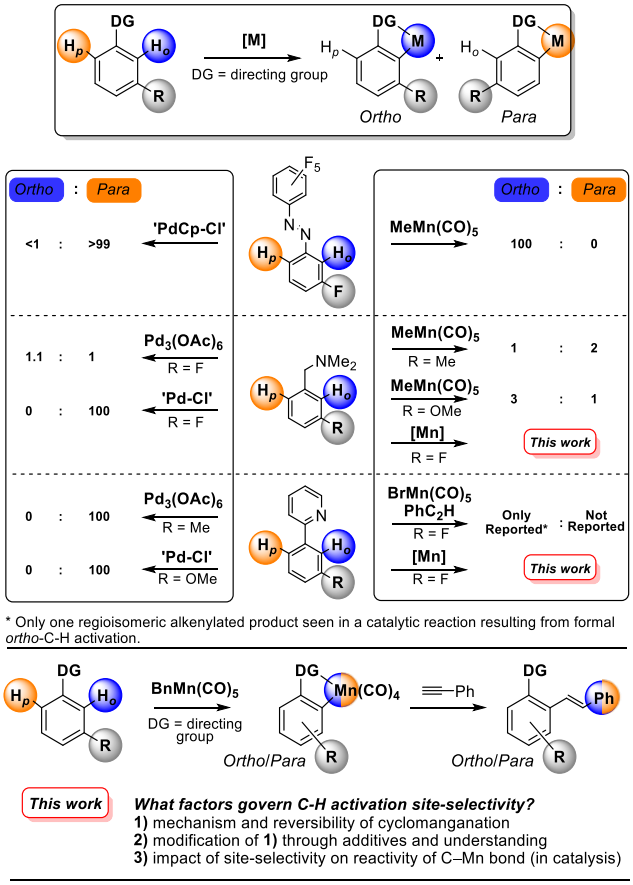

* Only one regioisomeric alkenylated product seen in a catalytic reaction resulting from formal *ortho*-C-H activation.

Scheme 1. Cyclometallation examples where there is a regiochemical choice impacted by fluorine substituents in C–H bond activation and functionalization processes.

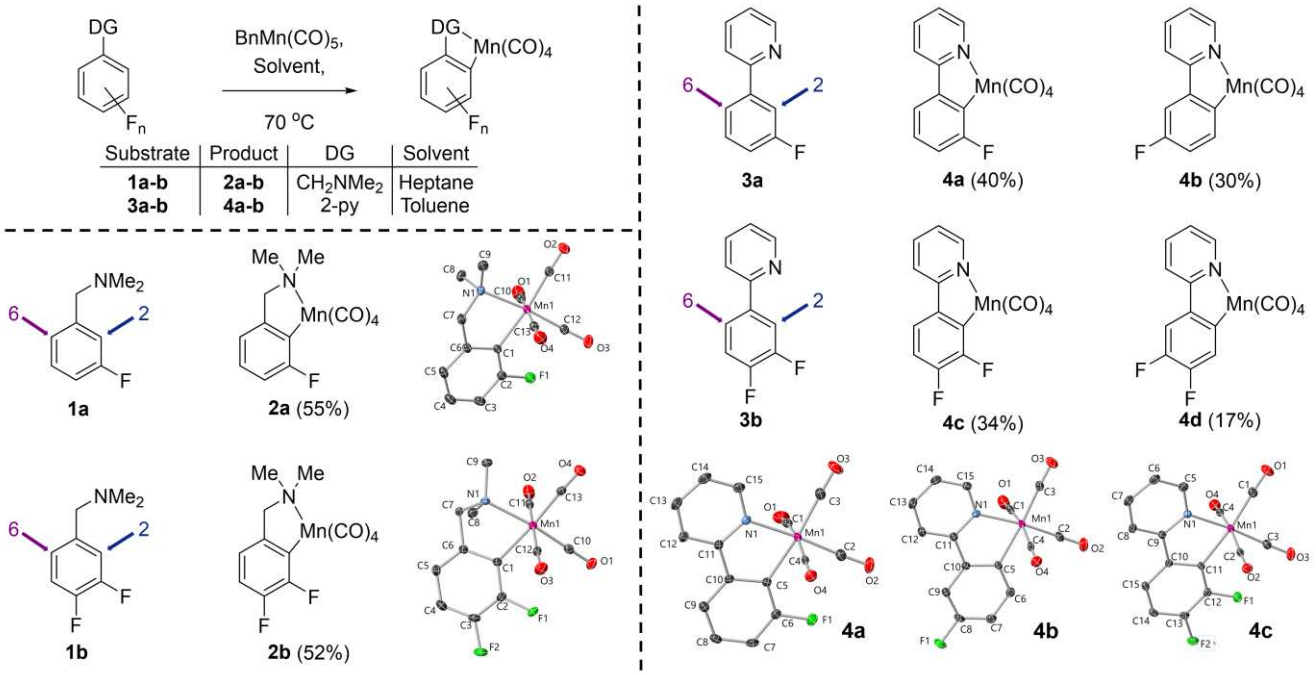

Scheme 2. Cyclomanganation of fluorinated benzylamines and 2-phenylpyridines.

These methods offer an opportunity to rationalize the kinetic and thermodynamic control exerted by the incorporation of fluorine into substrates for Mn-catalyzed C–H bond functionalization.

Herein we describe the *ortho*-selective C–H bond metalation of *meta*-fluorinated benzylamine and 2-phenylpyridine derivatives, where we aim to:

- Measure the extent of the fluorine-induced regioselectivity in relevant aromatic systems.
- Assess the origin of the *ortho*-fluorine effect in a *3d*-metal system through understanding of the reaction mechanism and the properties affecting activation of C–H bonds, including the role of additives.

RESULTS AND DISCUSSION

Two sets of substrates were selected to investigate the nature of the *ortho*-fluorine effect in cyclomanganation reactions. *Meta*-fluorinated benzylamines were chosen as they enable comparison with other Mn(I)-mediated reaction systems using different substituents (Me, OMe),[5c] as well as our previously reported results on the corresponding cyclopalladation processes.[5d] The reaction can either react to form the C–Mn bond at the 2 or 6 position of the arene (Scheme 2) which will be referred to as *ortho* and *para* respectively, *i.e. ortho* or *para* to the substituent (*i.e.* the directing group). Due to the extensive use of 2-phenylpyridines in Mn(I)-catalyzed C–H bond functionalization[8,9,12,16] and our previous mechanistic studies into these reaction systems,[14,15,17] the cyclomanganation of fluorinated 2-phenylpyridines **3a** and **3b** were investigated (Scheme 2). Related studies on ligands with a pyrrolidine directing group are reported in the Supporting Information.

The cyclomanganation of monofluorinated benzylamine derivative **1a** was performed using $BnMn(CO)_5$ as the manganese precursor in hexane at reflux for 16 hours (Scheme 2). The ^{19}F NMR spectrum of the crude reaction mixture revealed that only one regioisomer of the manganacycles was generated in substantial quantities, with the minor regioisomer only being present in trace amounts (< 1%). Following purification (55% yield of isolated material) and subsequent characterization, it was determined that the major regioisomer in the reaction was *ortho*-complex **2a**. Single crystal X-ray diffraction (XRD) analysis was utilized to provide further support for the structural assignment. Thus, the reaction exhibited similar *ortho*-preference as reported for the cyclomanganation of fluorinated azobenzenes.[5b] Repeating the cyclomanganation on difluorinated derivative **1b** yielded *ortho*-complex **2b** as the major product (99:1, *ortho*:*para*). The yield of the reaction (52%) was also comparable to **1a**, showing that the additional fluorine substituent had a limited effect on both the selectivity and efficiency of the reaction.

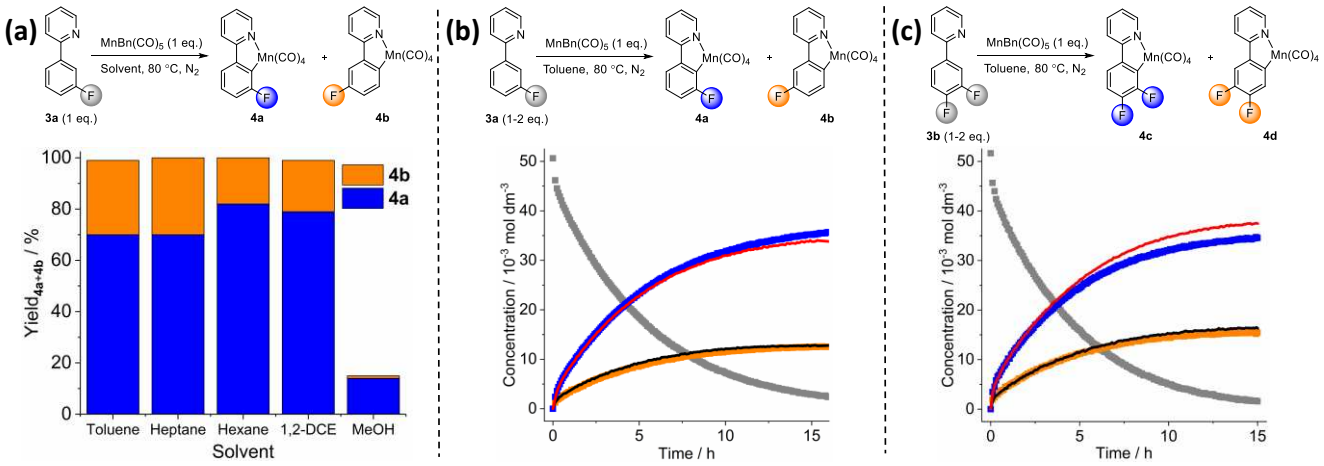

Figure 1. (a) Solvent screen for the cyclomanganation of **3a**. (b) *In situ* ^{19}F NMR study of the cyclomanganation of **3a** using $C_6H_5CF_3$ as internal standard. Key: blue/red lines = **4a** using 1.0 (blue) and 1.5 eq. (red) **3a** and orange/black lines = **4b** using 1.0 (orange) and 1.5 eq. (black) **3a**. (c) *In situ* ^{19}F NMR study of the cyclomanganation of **3b**. Key: blue/red lines = **4c** using 1.0 (blue) and 1.5 eq. (red) **3b** and orange/black lines = **4d** using 1.0 (orange) and 2.0 eq. (black) **3b**.

The alkyl substituents on the amine proved to have limited impact on the reaction, as when the dimethylamino group was altered to a pyrrolidine ring, the reaction again generated the *ortho*-complexes as the major product in comparable yields (see Supplementary Information). However, the extent of the *ortho*-preference was reduced marginally to 93:7, *ortho*:*para*, for the monofluorinated derivative. The cyclomanganation of *meta*-fluorinated 2-phenylpyridine **3a** was performed using the same manganese precursor, $BnMn(CO)_5$, in toluene at 80 °C for 16 hours. The crude ^{19}F NMR spectrum revealed complete consumption of **3a** and the presence of two new fluorine-containing species. Following purification, both the *ortho*- (**4a**, 40%) and *para*-isomers (**4b**, 30%) of the manganacycle were characterized. Due to difficulties in the separation of the regioisomeric complexes, the ratio of isolated material does not reflect the true ratio of the reaction (see further details below). Nevertheless, the relatively large quantities of *para*-complex **4b** presented a marked difference in reactivity and selectivity as compared to the benzylamines and other *ortho*-selective directing groups. The extensive formation of the *para*-complex was mirrored in the cyclomanganation of difluorinated 2-phenylpyridine **3b**, yielding both the *ortho*- (**4c**, 34%) and *para*-complexes (**4d**, 17%).

Single crystal XRD analysis for manganese(I) complexes **4a-c** (see Supplementary Information) showed no significant difference in the C_{Ar}–Mn bond lengths between the two regioisomers (**4a** = 2.0557(18) Å and **4b** = 2.0510(17) Å), consistent with Davies and Macgregor's study on *ortho*/*para*-cyclometallated (M = Rh and Ir) 1-phenylpyrazoles.[5a] This finding suggested that the relative strength of the C–Mn bond was not responsible for the observed regioselectivity. In addition, the Mn–CO bond lengths and relative bond angles were also similar between the two regioisomers. The two species additionally exhibited similar IR spectra, with only minor shifts in the metal carbonyl bands (**4a** = 2077, 1992 (br) and 1934 cm^{-1} and **4b** = 2081, 1995 (br) and 1942 cm^{-1} in CH_2Cl_2 at room temperature). The C_{Ar}–Mn bond length was not altered when adding another fluorine substituent (**4c** = 2.0501(12) Å) and no significant change could be found in the other relevant bond lengths and bond angles.

***In situ* ^{19}F NMR reaction monitoring.** The unusually small *ortho*-selectivity for the 2-phenylpyridine derivatives **3a** and **3b** warranted further investigation to determine the rationale behind the lower selectivity and to understand the difference in reactivity when other directing groups, such as the benzylamines, were employed.

Initially, to determine if any effects had arisen from the reaction solvent, a solvent screen was completed for the cyclomanganation of **3a** (Figure 1a). The reactions were performed at 80 °C for 16 hours, after which time the crude material was analyzed by ^{19}F NMR spectroscopic analysis. Both high boiling point hydrocarbon solvents, toluene and heptane, exhibited complete consumption of **3a** and a similar *ortho*/*para* ratio of 7:3 (**4a**/**4b**). Changing to a lower boiling point solvent in hexane led to reduced formation of *para*-complex **4b** (4.6:1, **4a**/**4b**), though still affording complete consumption of **3a**. A similar reactivity and *ortho*/*para* ratio (4:1) was obtained when the cyclomanganation was performed in 1,2-dichloroethane (1,2-DCE).

A major change in reactivity was observed with MeOH and extensive manganese degradation was noted, with only minor quantities of the manganacycles generated with a strong preference for *ortho*-complex **4a** (14:1, **4a**/**4b**). Toluene was selected as the reaction solvent for the subsequent studies due to the high efficiency of the reaction and relatively large amount of *para*-complex **4b** that was formed. The reaction kinetics of the cyclomanganation reaction in toluene at 80 °C using monofluorinated substrate **3a** were monitored using *in situ* ^{19}F NMR spectroscopic analysis (Figure 1b). The clear difference in chemical shift between the regioisomers (**4a** = −86.3 ppm and **4b** = −121.4 ppm) allowed for the reaction profile for each product to be obtained. The *ortho*/*para* ratio of 2.9:1 remained constant throughout the reaction and no significant degradation or interconversion between the species could be observed following completion of the reaction. The observed rate of formation of both products (k_{4a} = 5.1 ± 0.6 10^{-5} s^{-1} and k_{4b} = 5.6

± 0.1 10^{-5} s^{-1}, Table 1) was near identical to the loss of starting material (k_{3a} = 5.20 ± 0.07 10^{-5} s^{-1}), which is expected for parallel reaction pathways in such systems.[18]

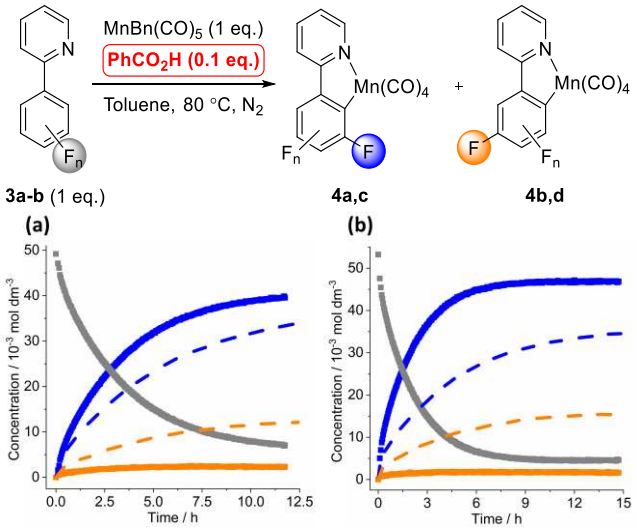

Figure 2. Cyclomanganation of fluorinated 2-phenylpyridine derivatives **3a**-**b** with the addition of $PhCO_2H$ (0.1 eq.), and the kinetic trace obtained by *in situ* ^{19}F NMR spectroscopy using $C_6H_5CF_3$ as internal standard. Key: dotted line = without additive and squares = with $PhCO_2H$ added. (a) Kinetic trace for the reaction using **3a**. (b) Kinetic trace for the reaction using **3b**.

The lack of interconversion between **4a** and **4b** indicated an irreversible reaction mechanism, which could be affected by the addition of excess **3a**. Thus, the reaction was repeated using 1.5 equivalence of **3a** relative to $MnBn(CO)_5$ (Figure 1b). The reaction profile and regioselectivity (2.6:1, **4a**/**4b**) was near identical to the reaction with 1 equivalent (2.9:1, **4a**/**4b**), suggesting a zero-order dependence in **3a** on the reaction and that **3a** did not impact the reversibility of the reaction. Consequently, the apparent irreversibility of the reaction inferred that the regioselectivity was kinetically determined and provided an explanation for the observed selectivity between the two regioisomeric complexes even with near identical C–Mn bond lengths.

When the reaction was repeated using two equivalents of $BnMn(CO)_5$ (see Supplementary Information) the observed rate constant almost doubled (k_{4a} = 9.3 ± 0.5 × 10^{-5} s^{-1}), while the *ortho*/*para* ratio remained similar (2.2:1, **4a**/**4b**). This increase in the rate of reaction suggested a first order dependence of manganese in the reaction, likely derived from the initial loss of a CO-ligand as being rate-limiting.

The cyclomanganation of **3b** (Figure 1c) exhibited a similar kinetic trace to **3a**, with a minor shift in the *ortho*/*para* ratio (2.3:1). Again, no significant interconversion could be observed at longer times following completion of the reaction, even after 40 hours (see Supplementary Information). Repeating the reaction with excess **3b** (2 equivalents) again yielded a similar reaction profile.

Effect of acid additives. We have previously shown that carboxylic acid additives have a marked effect on the efficacy of Mn(I)-catalyzed C–H bond functionalization reactions,[17c] enabling ligand liberation from cyclomanganated 2-phenylpyridines.[15] Hence, it was hypothesized that addition of an acid would enable a reversible reaction mechanism for C–H bond activation through a protodemetallation pathway, in a similar vein to that observed for a half-sandwich Rh complex reported by Jones and co-workers.[19] The addition of a carboxylic acid additive could potentially result in a mechanistic shift for cyclomanganation from σ-Complex-Assisted Metathesis (σ-CAM) to a CMD/AMLA-6 mechanism.[17]

Table 1. Observed rate constants for the formation of *ortho*-complexes **4a** and **4c**.

Entry	Substrate (eq.)	k_{ortho} / 10^{-5} s^{-1}	*o*/*p* selectivity
1	**3a** (1)	5.1 ± 0.6	2.9
2	**3a** (1.5)	5.2 ± 0.1	2.6
3	**3a** (1)[a]	9.3 ± 0.5	2.2
4	**3b** (1)	5.9 ± 0.1	2.3
5	**3b** (2)	5.9 ± 0.1	2.5
6	**3a** (1)[b]	10.1 ± 0.1	17

[a] 2 equivalence of $BnMn(CO)_5$. [b] 0.1 equivalence $PhCO_2H$ added (entry 6, highlighted to show acid effect).

The cyclomanganation of **3a** with added benzoic acid (0.1 equivalence) resulted in a substantially different reaction profile (Figure 2a), with *ortho*-complex **4a** formed in a large excess over **4b** (17:1). At no point during the reaction did the concentration of **4b** reach a significant level in comparison to **4a**. Unreacted **3a** (14%) was observed in the solution at the end of the reaction, yielding a final **3a**/**4a**/**4b** ratio of 3:17:1. Addition of benzoic acid (0.1 equivalence) to the cyclomanganation of **3b** (Figure 2b) resulted in an increased selective reaction to afford the *ortho*-complex **4c** preferentially over **4d** (29:1 ratio). A small amount of **3b** remained in solution (3%), following completion of the reaction, but in lower quantities than for the monofluorinated derivative.

The addition of benzoic acid to the cyclomanganation reactions increased the rate of the reaction (k_{4a} = 5.20 ± 0.07 × 10^{-5} s^{-1} without additives and k_{4a} = 1.01 ± 0.01 × 10^{-4} s^{-1} with 0.1 eq (Table 1). benzoic acid added), consistent with a shift to a CMD/AMLA-6 mechanism. Performing the experiments at a range of acid concentrations (0.05–0.20 eq.) led to a linear increase in the observed rate of C–Mn bond formation (see Supplementary Information). The plot of ln(k_{4a}) *vs* time yielded a surprising reaction order in acid of 0.44 ± 0.02, which likely stems from the operation of both σ-CAM and CMD/AMLA-6 mechanisms under the reaction conditions.

To further probe the effect of the acid additive, *para*-complex **4b** was heated in toluene and monitored by *in situ* ^{19}F NMR spectroscopic analysis (Figure 3). The reaction showed no conversion to either **3a** or **4a** within the first

4.25 hours, consistent with an irreversible reaction mechanism and reveals the high thermal stability associated with these manganacycles. The addition of benzoic acid (0.5 equivalents) was followed by the rapid depletion of the resonance for **4b** and liberation of **3a** (67%) by protonation of the Mn-C bond and formation of **4a** (31%). Interestingly, **3a** was observed to form, reaching a steady level, prior to the generation of the *ortho*-complex **4a**. This indicates the presence of an intermolecular mechanism for interconversion of the two regioisomeric products. The relatively large amount of acid added explains why a protonated compound **3a** is formed under the reaction conditions.

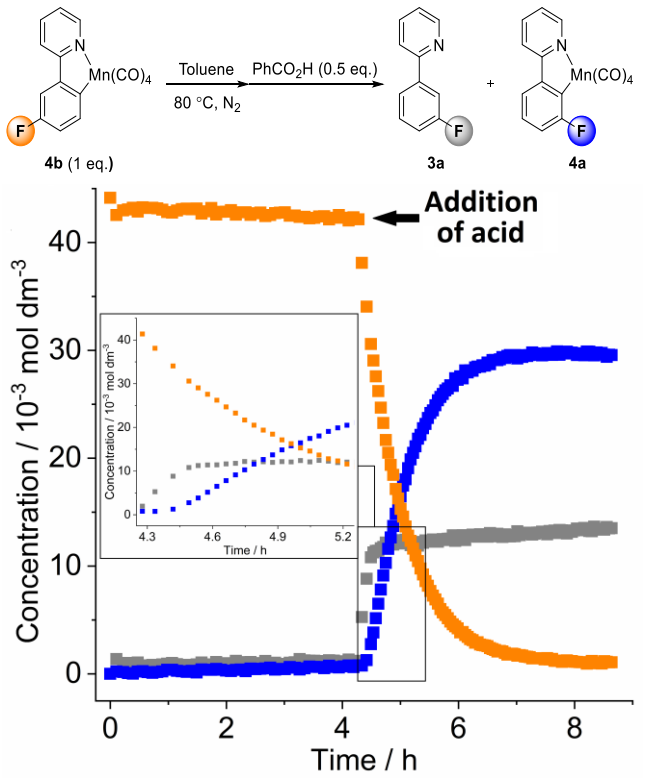

Figure 3. *In situ* ^{19}F NMR spectroscopic monitoring of the heating of **4b** at 80 °C in toluene, before addition of $PhCO_2H$ (0.5 eq.) after 4.25 h.

To assess the intra- *vs* intermolecular nature of the regioisomer interconversion (**4b** → **4a**), a competition experiment between *para*-fluorinated 2-phenylpyridine **3c** and **3a** was performed and monitored using *in situ* ^{19}F NMR spectroscopy (Figure 4). Initially, **3a** was cyclomanganated without any additives, thereafter **3c** (0.6 equivalents) and benzoic acid (0.5 equivalents) was added to the reaction (Addition 1). *Meta*-complex **4e** was observed forming following this addition, suggesting the presence of an intermolecular reaction mechanism. The formation of **4e** was at the expense of both **4a** and **4b**, giving rise to a relative product ratio of 2.6:1 (**4a**/**4e**). Only a minor quantity of *para*-complex **4b** (3%) was present in the solution, and uncoordinated ligand **3a** was generated in the reaction because of the disappearance of **4a** and **4b**. A further 3.7 equivalents of **3c** were added (Addition 2) to the reaction following stabilization of the kinetic traces, leading to **4e** becoming the dominant manganacycle in a 2.7-fold excess over **4a** (0.375:1 **4a**/**4e**). **4b** only remained in trace quantities at the end of the experiment. The ratio between **3a** and **3c** (bound and free ligand) was 1.8:1 after Addition 1, which changed to 0.235:1 following Addition 2. The data support an CMD/AMLA-6 intramolecular protonation reaction, which is then followed by an intermolecular exchange between free and coordinated 2-phenylpyridine ligands.

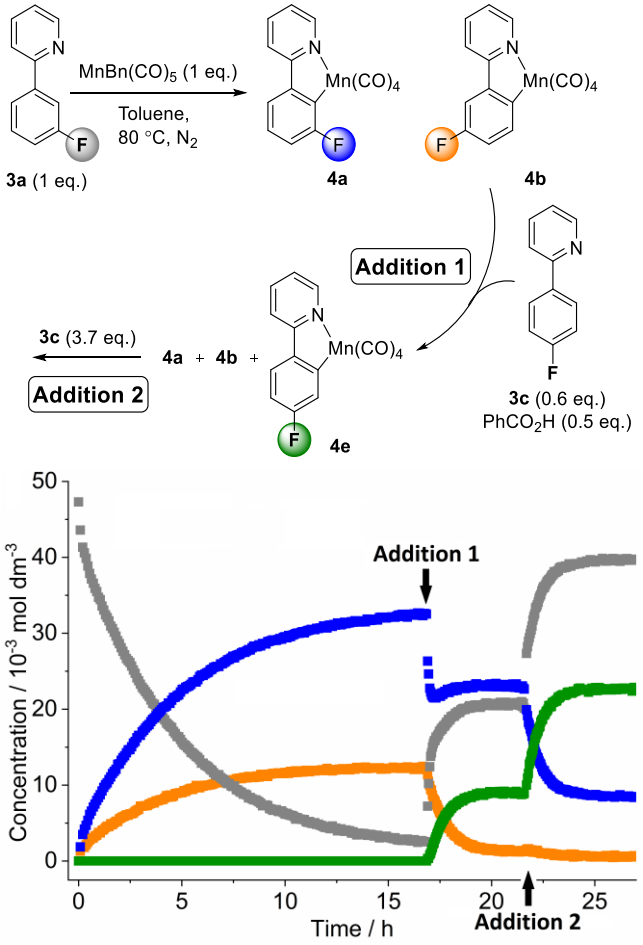

Figure 4. *In situ* ^{19}F NMR spectroscopic study, over the course of the cyclomanganation of **3a** at 80 °C in toluene, with addition of $PhCO_2H$ (0.5 eq.) and **3c** (0.6 + 3.7 eq.) after 17 and 21.5 h.

The distribution between the different complexes under these reversible reaction conditions should be determined by their relative thermodynamic stability. Thus, by comparing the quantity of each complex with the total amount of the corresponding 2-phenylpyridine derivative in solution, it was determined that *ortho*-complex **4a** was 1.4–1.6 times more stable than *meta*-complex **4e**. Due to the small amounts of *para*-complex **4b** in solution, a value for the relative stability of this complex could not be obtained. However, **4b** was clearly the least stable complex. The relative stability of the regioisomeric complexes can be summarized as **4a** > **4e** > **4b** (*ortho* > *meta* > *para*).

Time-Resolved Multiple Probe Spectroscopy monitoring of C–C bond formation. Having established the relative kinetic and thermodynamic preference in the C–H bond activation *in operando*, we sought to examine the influence of the fluorine atom in the organic ligand on further reactivity

of the regioisomeric manganacycles. Time-Resolved Multiple Probe Spectroscopy (TR^{M}PS) allows for the observation of light-induced events on picosecond to millisecond timescales. We have successfully employed this technique in studying several Mn(I)-mediated systems in recent years,[14,15,20] including solvent interactions following CO-loss[20a] and C–C bond formation with alkynes and other unsaturated substrates.[14] We thus identified TR^{M}PS-IR as a suitable technique to further explore the stability and reactivity of the regioisomeric manganacycles. TRMPS-IR is a pump-probe method in which a laser pulse (λ = 355 nm) induces the CO-loss from the Mn center and a subsequent IR pulse allows for the vibrational spectra of the resulting photoproducts to be obtained. The position and intensity of band due to the remaining CO-ligand provide information about the speciation and dynamic behavior following irradiation. We decided to utilize the alkyne insertion chemistry previously studied[14] as a probe for a potential kinetic *ortho*-fluorine effect in the C–C bond formation event. Changes in the rate of insertion of a substrate into the C–Mn bond should be indicative of any effects caused by the presence of fluorine.

Initially, *ortho*-complex **4a** was dissolved in neat PhC_2H and subsequently irradiated (λ = 355 nm) while monitored using TR^{M}PS-IR. The experiment used pump-probe delays between 1 ps – 800 μs and spectral detection in the region 1850–2100 cm^{-1}. The resulting data are presented as difference spectra (Figure 5), where positive peaks corresponding to the generated photoproducts and negative peaks to the ground state spectrum of **4a** following consumption by photolysis. The spectroscopic features and band locations for the various species mirrored those observed for the non-fluorinated derivatives (Table 2).[14] Light-induced loss of CO is evident at the shortest pump-probe delays employed (1 ps) and an arene-bound PhC_2H complex **5a** (1915 and 2016 cm^{-1}), was observed which was assigned on the basis of our previous work.[14] After 1 ns, the bands due to **5a** had been replaced by those for alkyne-coordinated complex **6a** (1923, 1955 and 2018 cm^{-1}). Evidence for the subsequent insertion of the alkyne into the C–Mn bond to form 7-membered complex **7a** was obtained though the bands at 1897, 1924 and 2013 cm^{-1}. A minor unknown species (2002 cm^{-1}) also formed in the reaction concomitantly with **7a**, though in minor quantities, which did not seem to affect the formation of **7a**.

Essentially identical data were obtained for the respective C–C bond forming events for the other manganacycles (**4b**-**4e**), with only minor changes in band position (see Supplementary Information) being observed. However, the presence of the fluorine substituents in were found to have a distinct impact on the rate of formation of compound class **7** (Table 1). When the 2-phenylpyridine ligand contained an *ortho*-fluorine substituent, the rate constant for the insertion of the alkyne into the Mn–C bond was reduced (*e.g.* for *ortho*-derivative **7a** $k_{insert} = 2.21 \pm 0.04 \times 10^4\ s^{-1}$; for the non-fluorinated derivative $k_{insert} = 1.35 \pm 0.09 \times 10^5\ s^{-1}$.[14] The addition of a second fluorine in **4c** and **4d** lowered the observed rate constant by factors of 6.1 and 3.1 respectively, compared to the mono-fluorinated derivatives (**4a** and **4b**).

The location of the fluorine substituents on the arene strongly influenced the observed rate constant for C–C bond formation: *para*-complex **4b** ($k_{insert} = 5.7 \pm 0.2 \times 10^4\ s^{-1}$) reacted faster than *ortho*-complex **4a** ($k_{insert} = 2.21 \pm 0.04 \times 10^4\ s^{-1}$). The rate constant obtained for *meta*-complex **4e** was located at an intermediate value when compared to the other two regioisomers ($k_{insert} = 3.5 \pm 0.1 \times 10^4\ s^{-1}$) and thus generated a relative reaction trend of **4b** > **4e** > **4a** (k_{insert}: *para* > *meta* > *ortho*), which in reverse mirrored the relative thermodynamic stability of the complex determined *vide supra*. These results unambiguously demonstrate the influence of the fluorine substituent on the rate of carbon-carbon bond formation with the coordination sphere of Mn(I) compounds.

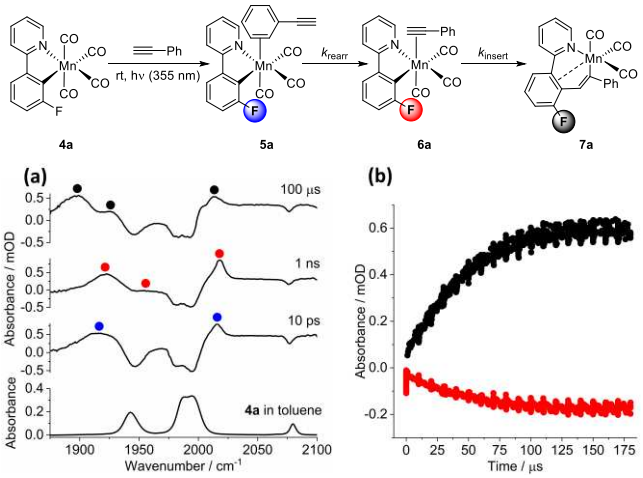

Figure 5. Reaction scheme and TR^{M}PS data for the 355 nm irradiation of **4a** in neat PhC_2H. (a) Ground state IR spectra of **4a** and IR spectrum over time of the reaction solution. (b) Kinetic trace for the C–C bond formation step. Red shows the growth and loss of the alkyne complex **6a** and black the growth of **7a**.

Catalytic reaction conditions. To gain further understanding of the influence of the fluorine substituents on the regioselectivity in catalytically relevant systems we studied the Mn(I)-mediated C–H bond alkenylation of the fluorinated 2-phenylpyridines. Mn(I)-catalyzed alkenylation processes have been extensively studied[8,9,12,14,17] and we have previously determined a full mechanism for this reaction.[17a] Chen and Wang reported the *ortho*-alkenylated 2-phenylpyridine **8a** as the sole reaction product when **3a** was used as a substrate,[9] and thus suggest that the cyclomanganation steps may be reversible under the reaction conditions. However, when we performed the reaction between PhC_2H (1 eq.) and **3a** (2 eq.) at 80 °C in toluene, using Cy_2NH (20 mol%) as base additive and $BrMn(CO)_5$ as pre-catalyst (Scheme 3), we isolated and characterized both the *ortho*- (**8a**, 68%) and *para*-alkenylated (**8b**, 9%) derivatives. The small quantities of **8b** generated in combination with change of solvent and reaction vessel may help explain the discrepancies in observed product ratio between our and Chen and Wang's work.[9]

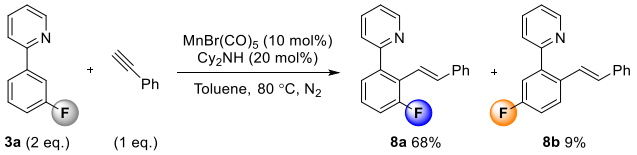

Scheme 3. Mn(I)-catalyzed alkenylation of **3a** using PhC_2H.

When benzylamine **1a** was exposed to the alkenylation conditions no alkene product was generated, only starting material was observed and no other products being observed in the crude ^1H and ^{19}F NMR spectra.

The strong and distinct IR-spectroscopic reporter ligands on the manganese allowed for the *in situ* monitoring of changes in metal carbonyl peaks under the catalytic conditions, and thus any new Mn-species generated, using a Mettler-Toledo ReactIR® instrument with Si-probe. We combined the *in situ* IR monitoring with *ex situ* ^{19}F NMR spectroscopy to obtain kinetic profiles, enabling distinction between different regioisomeric products and complexes with a 2-phenylpyridine moiety.

Several new manganese carbonyl species were observed to form during the reaction between PhC_2H (1 eq.) and **3a** (2 eq.) at 80 °C in toluene solution, using Cy_2NH (20 mol%) as base additive and $MnBr(CO)_5$ as pre-catalyst (Figure 6a). The pre-catalyst had been consumed within the first few minutes of the reaction and replaced by a new species (**7a'**, 1943, 1987 and 2071 cm^{-1}). The new species was assigned as the tetracarbonyl derivative of the 7-membered insertion complex **7a** due to its similarity to the non-fluorinated derivative, which we have previously characterized and shown to be the catalyst resting state.[17a] **7a'** displayed a single signal in the ^{19}F NMR spectra (−115 ppm) which exhibited the same kinetic profile as obtained from the *in situ* IR spectroscopy (Figure 6b). A ^{19}F NMR signal corresponding to *para*-derivative **7b'** was not found, suggesting that the *para*-complex is more active towards proton transfer. The concentration of **7a'** depleted slowly as the organic product formed; reaction completion was noted when no PhC_2H was left in solution. The remaining **7a'** was then rapidly consumed and replaced by *ortho*-complex **4a** *via* one of the available protonation pathways. *Para*-complex **4b** was not observed in the ^{19}F NMR spectra and highlighted a significant *ortho*-preference in the subsequent cyclomanganation step promoted by the excess 2-phenylpyridine in solution. It should be noted that the mechanism involving the PhC_2H acting as the acid may yield a different observed selectivity during the cyclomanganation step.[17a]

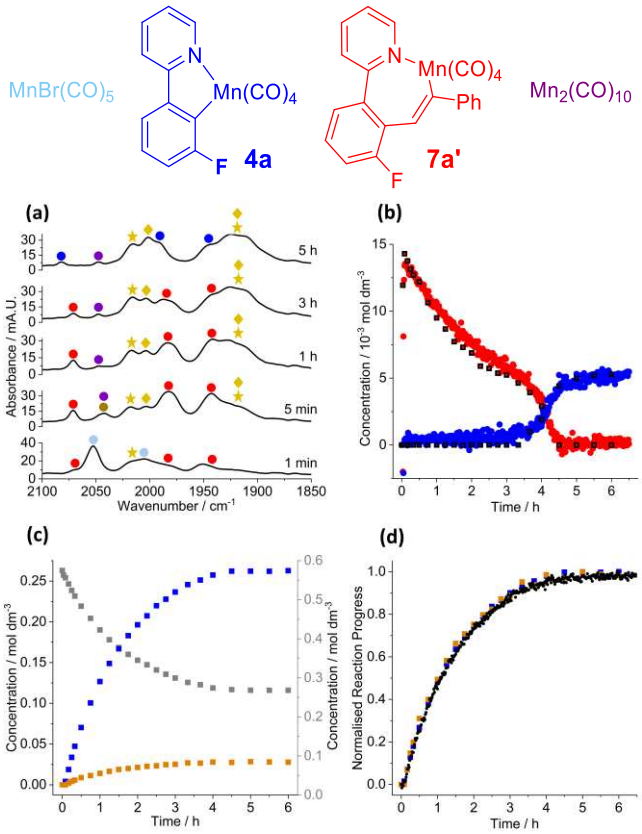

Figure 6. *In situ* IR and *ex situ* ^{19}F NMR spectroscopic monitoring of the alkenylation of **3a** (2 eq.) using PhC_2H (1 eq.), Cy_2NH (20 mol%), $MnBr(CO)_5$ (10 mol%) and *n*-Bu_2O. Key: see structures above and the gold star/diamonds represent manganese degradation complexes.

Manganese degradation complexes, such as Mn-clusters, were observed forming in the reaction in a similar fashion as observed in the non-fluorinated system.[17a] The exact structural identity of these Mn-clusters have not successfully been determined. A band at 2047 cm^{-1} was tentatively assigned as $Mn_2(CO)_{10}$, which we have previously observed under catalytic conditions,[17c] though the extensive spectral overlap did not allow for observation of the other spectroscopic bands corresponding to this species.

The kinetic profiles obtained by ^{19}F NMR spectroscopy (Figure 6c) showed that *ortho*-derivative **8a** was generated in 9-times excess over *para*-derivative **8b**. The shape of the curves was similar to that of the cyclomanganation reaction without acid additives (Figure 1b), though with a larger *ortho*-preference, suggesting an intrinsic formation of the organic products. This was further supported by the comparison between the normalized reaction profiles and an IR deformation band (970 cm^{-1}) corresponding to the alkene products (Figure 6d). The identical shape of the normalized reaction profiles demonstrates that the product ratio remained constant throughout the reaction and was not determined by secondary isomerization processes.

Table 2. TR^{M}PS data and rate constants for the C–C bond formation step in the photolysis of the manganacycles in neat PhC_2H. Scaled DFT-predicted vibrational modes are shown in italics. $\Delta G^{\ddagger}_{298.15}{}^{calc}$ is equivalent to the energy of **TS$_{67}$** (Scheme 4) and $\Delta G^{\circ}_{298.15}{}^{calc}$ the energy of **7**. In both cases, the energy of the respective complex **6** is taken as the reference energy. All energies are free energies at 298.15 K at the D3(BJ)-pbe0/def2-TZVPP//bp86/sv(p) level of theory.

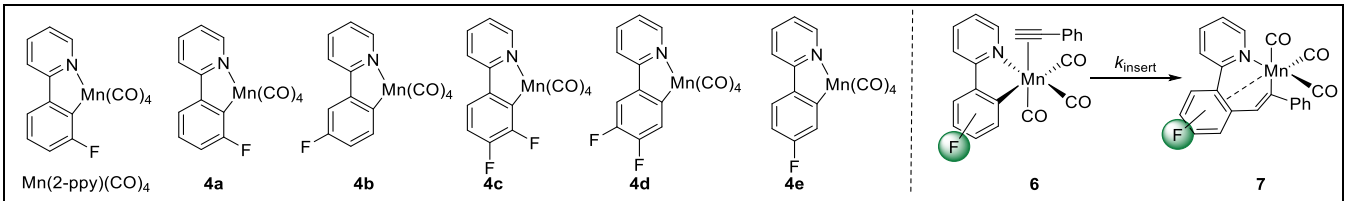

Entry	Compound	**6** / cm^{-1}	**7** / cm^{-1}	k_{insert} / 10^4 s^{-1}	$\Delta G^{\ddagger}_{298.15}$ / kJ mol^{-1} exp	$\Delta G^{\ddagger}_{298.15}$ / kJ mol^{-1} calc	$\Delta G^{\circ}_{298.15}$ / kJ mol^{-1} calc
1	Mn(2-ppy)(CO)$_4$	2009 *2010* 1944 *1941* 1912. *1915*	2008 *2003* 1922 *1925* 1899 *1893*	13.5 ± 0.9	44	29	-91
2	**4a**	2018 *2018* 1955 *1950* 1923 *1922*	2013 *2005* 1924 *1925* 1897 *1895*	2.21 ± 0.04	48	37	-83
3	**4b**	2013 *2012* 1948 *1942* 1912. *1917*	2011 *2003* 1920 *1925* 1897 *1895*	5.7 ± 0.2	46	35	-94
4	**4c**	2020 *2020* 1968 *1952* 1925 *1923*	2021 *2006* 1925 *1927* 1897 *1896*	0.86 ± 0.01[a]	51	43	-75
5	**4d**	2015 *2013* 1953 *1944* 1917 *1918*	2013 *2005* 1921 *1926* 1895 *1896*	1.86 ± 0.05	49	39	-88
6	**4e**	2014 *2013* 1950 *1944* 1916 *1918*	2012 *2003* 1923 *1926* 1898 *1896*	3.5 ± 0.1	47	37	-90

[a] Data treated with a 6-point smoothing function.

Therefore, the selectivity was likely set by the cyclomanganation step within the catalytic cycles, as the C–C formation step favors the generation of *para*-product **8b**. It was also possible that the protonation step would define the selectivity, but the lack of observation of the 7-membered catalyst resting state **7b'** likely means that the protonation was either favored for the *para*-isomer or similar between the two regioisomers

Computational work. Insight into how the incorporation of fluorine into the 2-phenylpyridine ligands affected both the kinetic and thermodynamics of complex formation was obtained through Density Functional Theory (DFT). The geometry of the complexes was optimized at the bp86/sv(p) level of theory and were used in subsequent single-point energy calculations at the D3(BJ)-pbe0/def2-TZVPP level. Thermal corrections (298.15 K) from the bp86/sv(p) level were then applied to obtain Gibbs free energies. This has proved to be a robust method to probe the chemistry of Mn-carbonyl compounds.[14,15,17,20]

A series of isodesmic reactions were modelled (Scheme 4a) to assess the thermodynamic effect of fluorine incorporation in the ligands. In this case, the change in Gibbs energy for substituting the parent 2-phenylpyridine by a range of fluorine-containing analogues (**3a-k**) was calculated.[21] Some general trends may be drawn from these data. Firstly, there is a thermodynamic preference for cyclomanganation at sites with an *ortho*-fluorine **(3a** and **3b**, blue arrows, **3f**, **3g**, **3i-k**, Scheme 4b) which results in a *ca*. 10 kJ mol^{-1} stabilization compared to the hydrogen-substituted analogue. Secondly, there is a small *meta*-fluorine effect which provides additional stabilization (*e.g.* **3g** and **3h**). Thirdly, the introduction of a *para*-fluorine (*e.g.* **3a** purple arrow, **3h**) does not appear to affect the overall stability. Although some of these changes in energy are relatively small, they are consistent across this series, and also the corresponding benzylamine analogues show an identical trend (see Supporting Information).

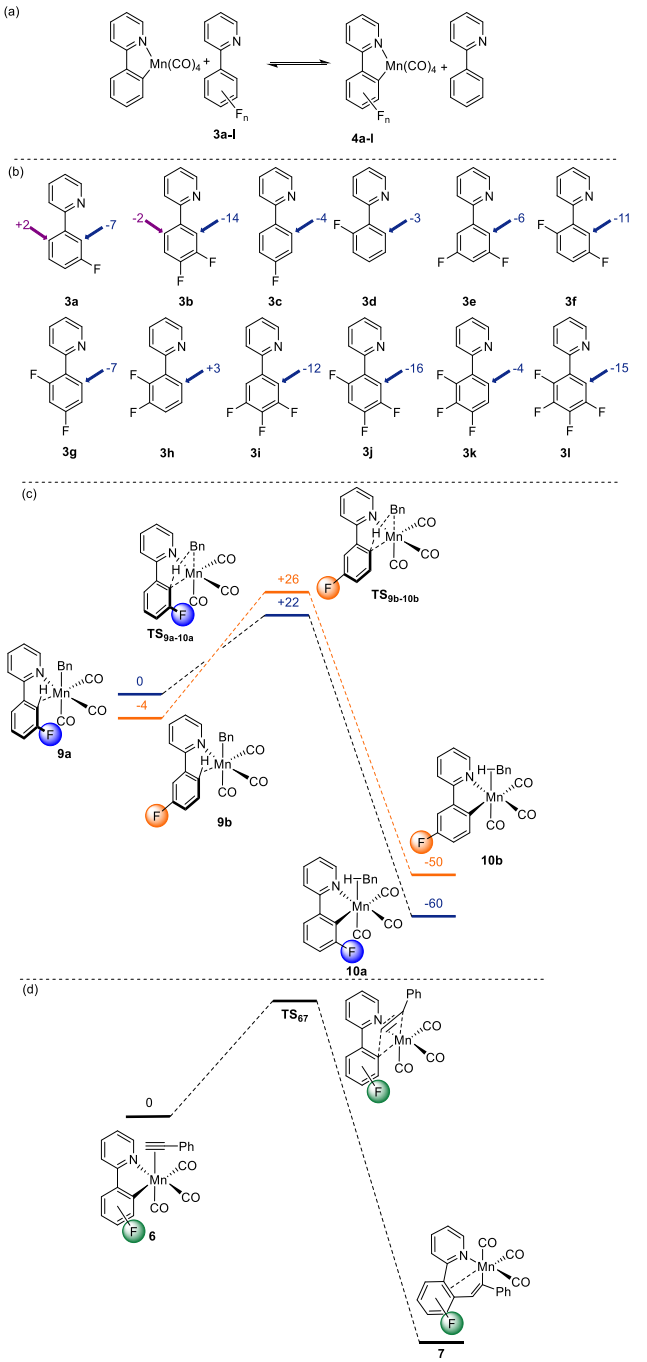

Scheme 4. (a) Isodesmic reaction used to probe the effect of fluorine incorporation into 2-phenylpyridine ligands (b) Calculated free energy changes at 298.15 K for the reaction shown in (a). The arrow shows the site of cyclomanganation (c) Reaction profile for the intramolecular C–H bond activation at Mn through a σ-CAM mechanism. (d) Calculated pathway for the insertion of PhC_2H into Mn–C bonds. Collated data are in Table 2. All energies are free energies at 298.15 K at the D3(BJ)-pbe0/def2-TZVPP//bp86/sv(p) level of theory.

The experimental data indicate that the reaction of $MnBn(CO)_5$ with **3a** shows only a small, kinetically controlled, *ortho*-fluorine effect with a **4a**:**4b** ratio of 7:3 in toluene solution. Insight into this process was obtained by modelling the two regioisomeric C–H bond activation pathways for **3a** by $MnBn(CO)_5$ (Scheme 4c). The computational model was based on coordination of **3a** to a "$MnBn(CO)_3$" fragment through the nitrogen of the pyridyl directing group and a C–H agostic interaction.[22] Two isomeric states **9a** (taken as the reference state) and **9b** were identified that differed only in the site of the agostic interaction. The C–H bond activation proceeds through $\mathbf{TS_{9\text{-}10}}$ in which the hydrogen atom is transferred to the benzyl ligand through a σ-CAM-type mechanism

In both cases, the barrier for this process is low indicating the mode of C–H bond activation is facile and would not be rate controlling. The energetic span for the formation of cyclomagnated complexes **10a** and **10b** is greater for **9b** (31 kJ mol^{-1}) compared to that for **9a** (23 kJ mol^{-1}) (assuming that **9a** and **9b** do not interconvert through a lower energy pathway) indicates a marginal kinetic preference for the formation of the *ortho*-fluorinated species. As with the calculations on the isodesmic reactions, **10a** containing an *ortho*-fluorine was located at lower energy than the *para*-substituted analogue **10b** (−60 kJ mol^{-1} vs −49 kJ mol^{-1}).

The insertion of PhC_2H into the Mn–C bond of **6** was also evaluated using DFT methods, again giving good agreement with the experiment outcomes (Table 2). In this case, the calculations indicated that the incorporation of fluorine into any position of the cyclomanganated phenyl ring increased the energy of the respective $\mathbf{TS_{6\text{-}7}}$ (Scheme 4d) (and thus $\Delta G^{\ddagger}_{298.15}{}^{calc}$) compared to the non-fluorinated analogue. The predicted change in free energies of activation span is 14 kJ mol^{-1} and so care must be taken in their interpretation. Of note there is essentially a linear correlation between the DFT-predicted barriers and those determined experimentally through time-resolved infra-red spectroscopy. This supports the interpretation that the incorporation of an *ortho*-fluorine atom decreases the rate of insertion. In addition, the substrates with the lowest rate of insertion also have the least negative calculated $\Delta G°_{298.15}{}^{calc}$ (that is the relative energy of **7** when compared to **6**). This may be interpreted as a further manifestation of the *ortho*-fluorine effect. In the case of complexes such as **4a** and **4c**, the formation of the respective complexes **7** results in the loss of a cyclomanganated atom with an *ortho*-fluorine, resulting in a lower the thermodynamic driving force for the reaction. This may be viewed as the *ortho*-fluorine stabilizing **6** which resulting in a higher kinetic barrier to insertion. If the insertion reaction is best viewed as an intramolecular nucleophilic attack on the coordinated alkyne and the presence of the *ortho*-fluorine may result in the phenyl group being a poorer nucleophile.

CONCLUSIONS

Controlling the site selectively of C–H bond activation in complex substrates is key to unlocking the potential of direct C-H bond functionalization methods. As recently highlighted by Davies and Macgregor, to draw robust mechanistic conclusions it is vital to understand if the selectivity of such a process is under kinetic or thermodynamic control.[6a,e] Through this study we have revealed the presence and varying strength of the *ortho*-fluorine effect in catalytically-competent Mn(I)-mediated C–H bond activation reac-

tions of fluorinated arenes. The irreversible reaction mechanism, and thus kinetically determined selectivity, under the standard reaction conditions afforded the *ortho*-complex of the benzylamine derivatives in near complete selectivity (**1a** and **1b**), while the *para*-complexes were more prevalent for the 2-phenylpyridine directed examples (**3a** and **3b**). By addition of benzoic acid, the mechanism could be altered to a reversible CMD/AMLA-6 mode of C–H bond activation and thereby ensuring the selectivity is determined thermodynamically. The relative thermodynamic stability determined by experimental and computational methods revealed an *ortho* > *meta* > *para* stability trend, which was the reverse of that observed for their reactivity towards C–C bond formation (*para* > *meta* > *ortho*), *i.e.* alkyne insertion into the C-Mn bond, as studied by Time-Resolved Multiple Probe Spectroscopy (TR^{M}PS). In combination with the single crystal XRD analysis it was determined that the inherent reactivity of the manganese(I) carbonyl complexes stems from their relative thermodynamic stability rather than other processes, such as their relative C–Mn bond strength.

The knowledge obtained was translated into the study of Mn(I)-catalyzed C–H bond alkenylation of 2-phenylpyridines, where the minor *para*-isomer **8b** was identified for the first time forming in minor amounts. The preference for *ortho*-isomer **8a** in the reaction was set by the cyclomanganation step within the catalytic cycles rather than by the *para*-favored C–C bond formation of the protonation step within the catalytic cycles. The outcome points to this being the most important step within the reaction mechanism if reactivity is to be altered to afford different regioselectivities or more efficient catalytic processes, *i.e.* lower Mn catalyst loadings.

AUTHOR INFORMATION

Corresponding Authors

J. M. Lynam - Department of Chemistry, University of York, York, YO10 5DD, UK http://orcid.org/0000-0003-0103-9479; Email: jason.lynam@york.ac.uk

I. J. S. Fairlamb - Department of Chemistry, University of York, York, YO10 5DD, UK http://orcid.org/0000-0002-7555-2761; Email: ian.fairlamb@york.ac.uk

Authors

L. Anders Hammarback - Department of Chemistry, University of York, York, YO10 5DD, UK http://orcid.org/0000-0003-1336-6848

Amy L. Bishop - Department of Chemistry, University of York, York, YO10 5DD, UK

Christina Jordan - Department of Chemistry, University of York, York, YO10 5DD, UK

Gayathri Athavan - Department of Chemistry, University of York, York, YO10 5DD, UK https://orcid.org/0000-0002-8948-8086

Jonathan B. Eastwood - Department of Chemistry, University of York, York, YO10 5DD, UK https://orcid.org/0000-0001-5586-7697

Thomas J. Burden - Department of Chemistry, University of York, York, YO10 5DD, UK https://orcid.org/0000-0001-9418-686X

Joshua T. W. Bray - Department of Chemistry, University of York, York, YO10 5DD, UK http://orcid.org/0000-0003-2384-9675

Francis Clarke - Department of Chemistry, University of York, York, YO10 5DD, UK

Adrian Whitwood - Department of Chemistry, University of York, York, YO10 5DD, UK https://orcid.org/0000-0002-5132-5468

Alan Robinson - Syngenta Crop Protection AG, Münchwilen, Breitenloh 5, 433, Switzerland

Jean-Philippe Krieger - Syngenta Crop Protection AG, Münchwilen, Breitenloh 5, 433, Switzerland

Ian P. Clark - Central Laser Facility, STFC Rutherford Appleton Laboratory, Harwell Science and Innovation Campus, Didcot, Oxfordshire OX11 0QX, U.K.

Michael Towrie - Central Laser Facility, STFC Rutherford Appleton Laboratory, Harwell Science and Innovation Campus, Didcot, Oxfordshire OX11 0QX, U.K.

ASSOCIATED CONTENT

Supporting Information

Included are the experimental procedures used, details of kinetic studies including time-resolved IR spectroscopic studies, and computational studies using density functional theory (DFT) methods (as a single PDF file). The Supporting Information is available free of charge on the ACS Publications website.

ACKNOWLEDGMENT

We are grateful to Dr. Jessica Milani for assistance with the synthesis of the fluorinated amine starting materials. We thank Professors Robin N. Perutz, Paul H. Walton and Andrew S. Weller (York) for discussion of our findings. We are grateful to the ERASUMS exchange scheme for funding C. J. and the Wild fund for supporting a PhD scholarship for G. A. Syngenta and EPSRC are thanked for funding an iCASE PhD studentship for L. A. H. We acknowledge EPSRC grants (EP/H011455, EP/K031589/1, EP/N509413/1).

REFERENCES

[1] (a) Kallane, S. I.; Braun, T. Catalytic Borylation of SCF_3-Functionalized Arenes by Rhodium(I) Boryl Complexes: Regioselective C–H Activation at the *ortho*-Position *Angew. Chem., Int. Ed.* **2014**, *53*, 9311–9315. (b) Carr, K. J. T.; Davies, D. L.; Macgregor, S. A.; Singh, K.; Villa-Marcos, B. Metal Control of Selectivity in Acetate-assisted C–H Bond Activation: An Experimental and Computational Study of Heterocyclic, Vinylic and Phenylic C(sp^2)–H Bonds at Ir and Rh. *Chem. Sci.* **2014**, *5*, 2340–2346. (c) Ciana, C.-L.; Phipps, R. J.; Brandt, J. R.; Meyer, F.-M.; Gaunt, M. J. A Highly Para-Selective Copper(II)-Catalyzed Direct Arylation of Aniline and Phenol Derivatives. *Angew. Chem., Int. Ed.* **2011**, *50*, 458–462. (d) Hartwig, J. F.; Larsen, M. A. Undirected, Homogeneous C–H Bond Functionalization: Challenges and Opportunities. *ACS Cent. Sci.* **2016**, *2*, 281–292.

[2] (a) Sambiagio, C.; Schönbauer, D.; Blieck, R.; Dao-Huy, T.; Pototschnig, G; Schaaf, P.; Wiesinger, T.; Zia, M. F.; Wencel-Delord, J.; Besset, T.; Maes, B. U. W., Schnürch, M. A Comprehensive Overview of Directing Groups Applied in Metal-Catalysed C–H Functionalisation Chemistry. *Chem. Soc. Rev.* **2018**, *47*, 6603–6743. (b)

Tang, R.-Y.; Li, G.; Yu, J.-Q. Conformation-Induced Remote *meta*-C–H Activation of Amines. *Nature* **2014**, *507*, 215–220. (c) Kuhl, N.; Hopkinson, M. N.; Wencel-Delord, J.; Glorius, F. Beyond Directing Groups: Transition-Metal-Catalyzed C–H Activation of Simple Arenes. *Angew. Chem., Int. Ed.* **2012**, *51*, 10236–10254.

[3] Ribas, X. C-H and C-X Bond Functionalization: Transition Metal Mediation; The Royal Society of Chemistry, 2013.

[4] Clot, E.; Eisenstein, O.; Jasim, N.; Macgregor, S. A.; McGrady, J. E.; Perutz, R. N. C–F and C–H Bond Activation of Fluorobenzenes and Fluoropyridines at Transition Metal Centers: How Fluorine Tips the Scales, *Acc. Chem. Res.* **2011**, *44*, 333–348.

[5] (a) Alharis, R. A.; McMullin, C. L.; Davies, D. L.; Singh, K.; Macgregor, S. A. The Importance of Kinetic and Thermodynamic Control when Assessing Mechanisms of Carboxylate-Assisted C–H Activation. *J. Am. Chem. Soc.* **2019**, *141*, 8896–8906. (b) Bruce, M. I.; Goodall, B. L.; Stone, F. G. A. Cyclometallation reactions. Part 17. Comparative Studies of the Manganation and Palladation of Some Substituted Azobenzenes. *J. Chem. Soc., Dalton Trans.* **1978**, 687–694. (c) Liebeskind, L. S.; Gasdaska, J. R.; McCallum, J. S.; Tremont, S. J. Ortho-Functionalization of Aromatic Ketones via Manganation. A Synthesis of Indenols. *J. Org. Chem.* **1989**, *54*, 669–677. (d) Milani, J.; Pridmore, N. E.; Whitwood, A. C.; Fairlamb, I. J. S.; Perutz, R. N. The Role of Fluorine Substituents in the Regioselectivity of Intramolecular C–H Bond Functionalization of Benzylamines at Palladium(II). *Organometallics* **2015**, *34*, 4376–4386. (e) Alharis, R. A.; McMullin, C. L.; Davies, D. L.; Singh, K.; Macgregor, S. A. Understanding Electronic Effects on Carboxylate-Assisted C–H Activation at Ruthenium: The Importance of Kinetic and Thermodynamic Control. *Faraday Discuss.* **2019**, *220*, 386–403.

[6] (a) Clot, E.; Besora, M.; Maseras, F.; Mégret, C.; Eisenstein, O.; Oelckers, B; Perutz, R. N. Bond Energy M–C/H–C Correlations: Dual Theoretical and Experimental Approach to the Sensitivity of M–C Bond Strength to Substituents. *Chem. Commun.* **2003**, 490–491. (b) Clot, E.; Oelckers, B; Klahn, A. H.; Eisenstein, O.; Perutz, R. N. *cis–trans* Isomerisation of $CpRe(CO)_2(H)(Ar_F)$ ($Ar_F = C_6F_nH_{5-n}$; n = 0–5) is the Rate Determining Step in C–H Activation of Fluoroarenes: a DFT Study. *Dalton Trans.* **2003**, 4065–4074. (c) Clot, E; Mégret, C.; Eisenstein, O.; Perutz, R. N. Exceptional Sensitivity of Metal-Aryl Bond Energies to *ortho*-Fluorine Substituents: Influence of the Metal, the Coordination Sphere, and the Spectator Ligands on M-C/H-C Bond Energy Correlations. *J. Am. Chem. Soc.* **2009**, *131*, 7817–7827. (d) Guihaumé, J.; Clot, E.; Eisenstein, O.; Perutz, R. N. Importance of Palladium–Carbon Bond Energies in Direct Arylation of Polyfluorinated Benzenes. *Dalton Trans.* **2010**, *39*, 10510–10519. (e) Lafrance, M.; Rowley, C. N.; Woo, T. K.; Fagnou, K. Catalytic Intermolecular Direct Arylation of Perfluorobenzenes. *J. Am. Chem. Soc.* **2006**, *128*, 8754–8756. (e) Selmeczy, A. D.; Jones, W. D.; Partridge, M. G; Perutz, R. N. Selectivity in the Activation of Fluorinated Aromatic Hydrocarbons by Rhodium Complexes $[(C_5H_5)Rh(PMe_3)]$ and $[(C_5Me_5)Rh(PMe_3)]$. *Organometallics* **1994**, *13*, 522–532. (f) He, M.; Soulé, J.-F.; Doucet, H. Synthesis of (Poly)fluorobiphenyls through Metal-catalyzed C-H Bond Activation/Arylation of (Poly)fluorobenzene Derivatives. *ChemCatChem* **2014**, *6*, 1824–1859.

[7] Pabst, T. P.; Obligacion, J. V.; Rochette, É.; Pappas, I.; Chirik, P. J. Cobalt-atalyzed Borylation of Fluorinated Arenes: Thermodynamic Control of C(sp^2)-H Oxidative Addition Results in *ortho*-to-Fluorine Selectivity, *J. Am. Chem. Soc.,* 2019, **141**, 15378–15389.

[8] Reviews: (a) Liu, W.; Ackermann, L. Manganese-Catalyzed C–H Activation. *ACS Catal.* **2016**, *6*, 3743–3752. (b) Cano, R.; Mackey, K.; McGlacken, G. P. Recent Advances in Manganese-Catalysed C–H Activation: Scope and Mechanism. *Catal. Sci. Technol.* **2018**, *8*, 1251–1266. (c) Hu, Y.; Zhou, B.; Wang, C. Inert C–H Bond Transformation Enabled by Organometallic Manganese Catalysis. *Acc. Chem. Res.* **2018**, *51*, 816–827.

[9] Zhou, B.; Chen, H.; Wang, C. Mn-Catalyzed Aromatic C–H Alkenylation with Terminal Alkynes. *J. Am. Chem. Soc.* **2013**, *135*, 1264–1267.

[10] For selected reviews concerning earth abundant catalysis in general, see: (a) Su, B.; Cao, Z.-C.; Shi, Z.-J. Exploration of Earth-Abundant Transition Metals (Fe, Co, and Ni) as Catalysts in Unreactive Chemical Bond Activations. *Acc. Chem. Res.* **2015**, *48*, 886–896. (b) Bedford, R. B. How Low Does Iron Go? Chasing the Active Species in Fe-Catalyzed Cross-Coupling Reactions. *Acc. Chem. Res.* **2015**, *48*, 1485–1493. (c) Wang, D.; Astruc, D. The Recent Development of Efficient Earth-Abundant Transition-Metal Nanocatalysts. *Chem. Soc. Rev.* **2017**, *46*, 816–854. (d) Albrecht, M.; Bedford, R. B.; Plietker, B. Catalytic and Organometallic Chemistry of Earth-Abundant Metals. *Organometallics* **2014**, *33*, 5619–5621. (e) Webster, R. L. β-Diketiminate Complexes of the First Row Transition Metals: Applications in Catalysis. *Dalton Trans.* **2017**, *46*, 4483–4498. (f) Kitanosono, T.; Masuda, K.; Xu, P.; Kobayashi, S. Catalytic Organic Reactions in Water toward Sustainable Society. *Chem. Rev.* **2018**, *118*, 679–746.

[11] (a) Bruce, M. I.; Iqbal, M. Z.; Stone, F. G. A. *ortho*-Metalation reactions. Part I. Reactions of Azobenzene with Some Metal Carbonyl Complexes of Sub-groups VI, VII, and VIII. *J. Chem. Soc. A* **1970**, 3204–3209. (b) Bruce, M. I.; Goodall, B. L.; Iqbal, M. Z.; Stone, F. G. A.; Doedens, R. J.; Little, R. G. *ortho*-Metallation of Benzylideneaniline: Structure of $C_6H_5N{:}CH{\cdot}C_6H_4Mn(CO)_4$. *J. Chem. Soc. D* **1971**, *0*, 1595–1596. (c) McKinney, R. J.; Firestein, G.; Kaesz, H. D. Metalation Reaction. VII. Metalation of Aromatic Ketones and Anthraquinone with Methylmanganese and Methylrhenium Carbonyl Complexes *Inorg. Chem.* **1975**, *14*, 2057–2061. (d) Bruce, M.; Goodall, B.; Matsuda, I. Cyclometallation Reactions. XIII. Reactions of Phenyl-substituted Heterocyclic Nitrogen-donor Ligands. *Aust. J. Chem.* **1975**, *28*, 1259–1264. (e) Robinson, N. P.; Main, L.; Nicholson, B. K. *Ortho*-manganated Arenes in Synthesis: V. *Ortho*-manganation of *N*-acyl Heteroaromatics, Benzamides and Substituted Benzaldehydes. Crystal Structure of (η^2-*O,C*-1-acetyi-2-indolyl)tetracarbonylmanganese. *J. Organomet. Chem.* **1988**, *349*, 209–218. (f) Pfeffer, M.; Urriolabeitia, E. P.; Fischer, J. Effects of *Ortho*-Substituents in the Synthesis and Stability of Cyclomanganated Benzylamine Derivatives. X-ray Crystal Structure of $Mn\{C_6H_2(OCH_3)_2\text{-}4,6\text{-}CH_2NMe_2\text{-}2\}(CO)_4$. *Inorg. Chem.* **1995**, *34*, 643–650.

[12] Wang, C. Manganese-Mediated C–C Bond Formation via C–H Activation: From Stoichiometry to Catalysis. *Synlett* **2013**, *24*, 1606–1613.

[13] (a) Liebeskind, L. S.; Gasdaska, J. R.; McCallum, J. S.; Tremont, S. J. Ortho-functionalization of Aromatic Ketones via Manganation. A Synthesis of Indenols. *J. Org. Chem.* **1989**, *54*, 669–677. (b) Cambie, R. C.; Metzler, M. R.; Rutledge, P. S.; Woodgate, P. D. Cyclomanganation of Diterpenoids; Functionalization of C14. *J. Organomet. Chem.* **1990**, *381*, C26–C30. (c) Tully, W.; Main, L.; Nicholson, B. K. Preparation of Cyclomanganated Chalcones and Their Reactions with Methyl Acrylate and Other α, β-Unsaturated Carbonyl Compounds. *J. Organomet. Chem.* **1995**, *503*, 75–92. (d) Depree, G. J.; Main, L.; Nicholson, B. K. Some Insertion Reactions of the Mn–C Bond of Cyclomanganated Triphenylphosphine Chalcogenides. *J. Organomet. Chem.* **1998**, *551*, 281–291. (e) Depree, G. J.; Main, L.; Nicholson, B. K.; Robinson, N. P.; Jameson, G. B. Synthesis and Alkyne-coupling Chemistry of Cyclomanganated 1- and 3-Acetylindoles, 3-Formylindole and Analogues. *J. Organomet. Chem.* **2006**, *691*, 667–679.

[14] Hammarback, L. A.; Clark, I. P.; Sazanovich, I. V.; Towrie, M.; Robinson, A.; Clarke, F.; Meyer, S.; Fairlamb, I. J. S.; Lynam, J. M. Mapping Out the Key Carbon–Carbon Bond-Forming Steps in Mn-Catalysed C–H Functionalisation. *Nat. Catal.* **2018**, *1*, 830–840.

[15] Hammarback L. A.; Aucott, B. J.; Bray, J. T. W.; Clark, I. P.; Towrie, M.; Robinson, A.; Fairlamb, I. J. S.; Lynam, J. M. Direct Observation of the Microscopic Reverse of the Ubiquitous Concerted Metalation Deprotonation Step in C–H Bond Activation Catalysis. *J. Am. Chem. Soc.* **2021**, *143*, 1356–1364.

[16] (a) Zhou, B.; Ma, P.; Chen, H.; Wang, C. Amine-Accelerated Manganese-Catalyzed Aromatic C–H Conjugate Addition to *α,β*-Unsaturated Carbonyls. *Chem. Commun.* **2014**, *50*, 14558–14561.

(b) Zhou, B.; Hu, Y.; Wang, C. Manganese-Catalyzed Direct Nucleophilic C(sp^2)–H Addition to Aldehydes and Nitriles. *Angew. Chem., Int. Ed.* **2015**, *54*, 13659–13663.

[17] (a) Hammarback, L. A.; Robinson, A.; Lynam, J. M.; Fairlamb, I. J. S. Mechanistic Insight into Catalytic Redox-Neutral C–H Bond Activation Involving Manganese(I) Carbonyls: Catalyst Activation, Turnover, and Deactivation Pathways Reveal an Intricate Network of Steps. *J. Am. Chem. Soc.* **2019**, *141*, 2316–2328. (b) Yahaya, N. P.; Appleby, K. M.; The, M.; Wagner, C.; Troschke, E.; Bray, J. T. W.; Ducket, S. B.; Hammarback, L. A.; Ward, J. S.; Milani, J.; Pridmore, N. E.; Whitwood, A. C.; Lynam, J. M.; Fairlamb, I. J. S. Manganese(I)-Catalyzed C–H Activation: The Key Role of a 7-Membered Manganacycle in H-Transfer and Reductive Elimination. *Angew. Chem. Int. Ed.* **2016**, *55*, 12455–12459 (c) Hammarback, L. A.; Robinson, A.; Lynam, J. M.; Fairlamb, I. J. S. Delineating the Critical Role of Acid Additives in Mn-Catalysed C–H Bond Functionalisation Processes. *Chem. Commun.* **2019**, *55*, 3211–3214.

[18] Hartwig, J. F. *Organotransition Metal Chemistry*; University Science Books, 2010.

[19] VanderWeide, A. I.; Brennessel, W. W.; Jones, W. D. Reversible Concerted Metalation–Deprotonation C–H Bond Activation by $[Cp^*RhCl_2]_2$. *J. Org. Chem*. **2019**, *84*, 12960– 12965,

[20] (a) Aucott, B. J.; Duhme-Klair, A.-K.; Moulton, B. E.; Clark, I. P.; Sazanovich, I. V.; Towrie, M.; Hammarback, L. A.; Fairlamb, I. J. S.; Lynam, J. M. Manganese Carbonyl Compounds Reveal Ultrafast Metal-Solvent Interactions. *Organometallics* **2019**, *38*, 2391–2401. (b) Aucott, B. J.; Eastwood, J. B.; Hammarback, L. A.; Clark, I. P.; Sazanovich, I. V.; Towrie, M.; Fairlamb, I. J. S.; Lynam, J. M. Insight into the Mechanism of CO-Release from Trypto-CORM Using Ultra-fast Spectroscopy and Computational Chemistry. *Dalton Trans.* **2019**, *48*, 16426–16436. (c) Eastwood, J. B.; Hammarback, L. A.; McRobie, M. T.; Clark, I. P.; Towrie, M.; Fairlamb, I. J. S.; Lynam, J. M. Time-resolved Infra-red Spectroscopy Reveals Competitive Water and Dinitrogen Coordination to a Manganese(I) Carbonyl Complex. *Dalton Trans.* **2020**, *49*, 5463–5470.

[21] In the case of monodentate ligands, the thermodynamic ortho-flourine effect is often quantified by determining changes to bond dissociation enthalpies. In this case, using this approach would involve either the cleavage of both Mn–N and Mn–C bonds of the bidendate ligands or, if just the Mn–C bond was broken, the formation of a diradical. Given the problems with both approaches, the isodesmic reaction model will give a more robust insight into the effect of fluorine incorporation, at least in this case.

[22] An alternative pathway in which C–H bond activation occurs at a "$MnBn(CO)_4$" was also located, see Supporting Information. In this case, **3a**, was coordinated through the pyridyl nitrogen and did not exhibit an agostic interaction. The transition state for C–H bond activation was found to be at much higher energy than that proceeding the σ-CAM mechanism in Figure 7c.

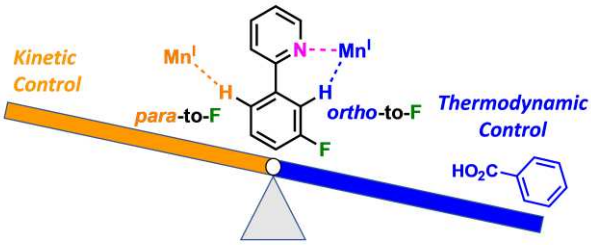

Table of Contents artwork